



ISSN: 2319-5967

ISO 9001:2008 Certified

International Journal of Engineering Science and Innovative Technology (IJESIT)

Volume 2, Issue 5, September 2013

# A Study of the Effect of Nozzle Spacing and Driving Pressure on the Water Jet Pump Performance

Tarek A. Meakhail<sup>1</sup>, Ibrahim R. Teaima<sup>2</sup>

Mechanical Power Engineering Department, Faculty of Energy Engineering, Aswan University,  
Aswan, Egypt

Researcher, Mechanical and Electrical Research Institute, National Water Research Center, Egypt

*Abstract— An extensive program has been made to study the effect of many geometric variables under different operating conditions on the performance of the jet pump at the National Water Research. This paper presents results of Computational Fluid Dynamic (CFD) analysis and experimental investigation of a water jet pump. The effect of driving pressure as well as the nozzle spacing has been investigated experimentally and numerically. Computational fluid dynamics (CFD) modeling studies were undertaken to understand the hydrodynamic characteristics with reference to the jet pump geometry. The CFD model also provides a basis for quantifying the effects of operating conditions on the pump performance. In this paper, the performance measurements are carried out for four driving pressures 1, 1.5, 2, and 2.5 bar, also four values of nozzle spacing to throat diameter ratio are used, they are  $X = 0, 0.5, 0.75$  and  $1$ . The results show that the important findings of velocity profile and pressure distributions are presented and discussed. The value of  $X$  that gives the maximum efficiency was found to be  $0.5$ . The liquid jet pump is increasingly prone to cavitation as the nozzle to throat spacing is reduced to zero. The CFD's results were found to agree well with actual values obtained from the experimental results*

*Index Terms— Jet pump, Driving pressure, Nozzle spacing, CFD.*

## I. INTRODUCTION

The liquid-liquid jet pump dates back to the application by Thompson [1] in 1852 and to the first theoretical developments by Rankine [2] in 1870 and Lorenz [3] in 1910. The theory of the jet pump was suggested by Gosline and O'Brien [4] who established the governing equations to represent the processes in jet pumps. This theory was later improved to include the friction losses by investigators like Cunningham and River [5] and Vogel [6]. Jet pump is a simple device applied widely in the fields of civil engineering to dewater foundation excavations in fine soils and dredging. It is also used in several mechanical, chemical, and industrial engineering applications for evacuating gases, lifting of liquids, and solid particles. The principle of the jet pump is to convert the pressure energy of the motive (primary) fluid into the velocity energy through driving nozzle. The resultant jet of high velocity creates a low pressure area in the suction chamber causing the pumped (secondary) fluid to flow into this chamber. Consequently, there is an exchange of momentum between the two streams in the mixing chamber resulting in a uniformly mixed stream traveling at an intermediate velocity between the motive and pumped fluid velocities. The diffuser is shaped to convert the kinetic energy of the mixture to pressure rise at the discharge flange with a minimum energy loss, as schematically shown in Fig. 1. The absence of moving mechanical parts eliminates the operational problems associated with bearings seals and lubrication. Therefore, such pumps are widely used because of their simplicity and high reliability (as a consequence of no moving parts).

There is large number of researches concerned with jet pumps. Among these researches, Mueller [7] carried out experiments on a water jet pump to determine the optimum dimensions of such pump. Reddy and Kar [8] carried out both theoretical and experimental studies. The experimental work in their research was divided into two parts: tests with the components and tests with an assembled jet pump. Cunningham [9] reviewed the nozzle spacing and mixing throat lengths. He showed a detailed tabulation of literature recommendation for the ratio of nozzle-to-throat spacing to mixing chamber diameter ( $x/D$ ). The results can be summarized by noting ( $x/D$ ) should be of the order of  $0.5$  to  $1.5$ . Although he showed this range, he suggested further study for the effect of ( $x/D$ ) on the performance and the mixing process in the mixing chamber. The ESDU design guide [10] suggested that the nozzle should be placed at a distance of  $0.5$  to  $1$  length of the mixing chamber's throat diameter upstream of the mixing chamber inlet. Aphornratana and Eames [11] showed very different study for a steam ejector, his optimum ( $x/D$ )

ratio was found in the range of zero to about 0.8 inside the mixing chamber. He explained that difference as the complex nature of flow structure, and it is difficult to give precise recommendations for the optimum nozzle position. Fan et al., [12] studied the optimization of jet pump design using computational fluid dynamics analysis. They design initial jet pump using an analytical approach and its efficiency was improved using an efficient and accurate computational fluid dynamics model of the compressible turbulent flow in the pump. They concluded that this prediction agreed well with corresponding experimental data. Parametric studies were performed to determine the influence of the pump's geometry on its performance and the high fidelity CFD solutions were used to build surrogate models of the pump's behavior using the moving least squares method. Global optimization was carried out using the surrogates. This approach resulted in pump efficiency increasing from 29% to 33% and enabled the energy requirements of the pump to be reduced by over 20%.

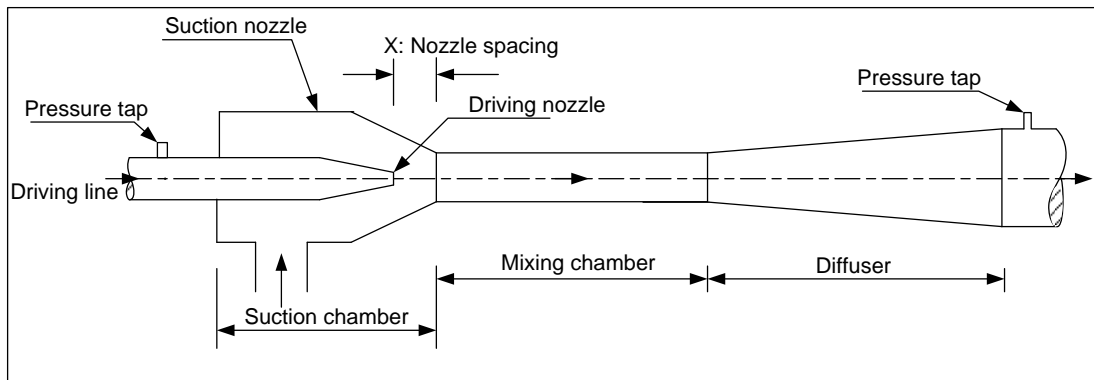


Fig. (1) Assembly of jet pump

With the development of computer hardware and numerical methodology, CFD tools are being used for better understanding of the mixing process, system design and performance evaluation considering the hydrodynamic performance. The advantages of this method are that it takes less time and cost than experimental method for predicting the performance of a jet pump. The second point is that CFD results can produce large volumes of results at virtually no added expense and it is very convenient to perform parametric research and optimization analysis. The third reason is that by experimental means, some parameters are difficult to be obtained. The last but not the least reason is the fundamental physics of the jet pump used in various fields are similar, so that other installations may be investigated too by utilizing this technique. More published work is presented by the author and co-workers in [13-19]. To the best knowledge of the authors, the effect of (x/D) ratio and driving pressure on the performance of the jet pump needs more research work. Therefore, in this current article, the effect these parameters on the performance is studied experimentally and numerically. The details of the test rig and all experimental procedures can be found in reference [19]. The performance of jet pump is generally considered to be a function of the parameters defined in the following:

i- Flow ratio  $M = \frac{Q_s}{Q_m}$  ,

ii- Head ratio  $N = \frac{(H_d - H_s)}{(H_m - H_d)}$ ,

iii- Efficiency,  $\eta$  = The ratio of the total energy increase of suction flow to the total energy increase of driving flow as ,

$$\eta = \frac{[Q_s \cdot (H_d - H_s)]}{[Q_m \cdot (H_m - H_d)]}, \quad \eta = M \cdot N$$

## II. NUMERICAL TECHNIQUE

Numerical computations are carried out by using CFX-TASCflow [20] code. This code solves the Reynolds averaged Navier–Stokes equations in primitive variable form. The standard  $k-\epsilon$  turbulence model is used to study the effect of turbulence of fluid flow. Very recent comparisons between CFD and experiments have shown that the standard  $k-\epsilon$  model is capable of predicting accurately the important global performance indicators, for subsonic, supersonic single and two phase flow, and that the main difference between turbulence models lies in

their prediction of local flow structure, Fan et al., [12] Hemidi et al., [21]. Also, in order to study the flow near wall; wall function is used to resolve the wall flows. This code uses a finite element based finite volume method. To achieve a convergent numerical solution, consistent and stable, as well as various numerical schemes have been implemented in the CFX-TASCflow code.

**A. Boundary conditions**

To get an accurate simulation, the same dimensions of the tested jet pump are used. As well, the boundary conditions of fluid flow are the same as that of the experimental work. The mass flow rate of each of the primary and secondary streams giving the correct mass flow ratio at the inlet and the outlet static pressure is set as outlet boundary conditions. The turbulent intensity and the eddy length are 0.03 and 0.03, respectively, while the average Reynolds number is  $7.0 \times 10^5$ . The maximum residuals are less than  $E-04$ . To reach a good convergence, the numbers of iterations are 150 for a time of calculation of about 3 hours on a core 2 duo processor, for each run. Table (1) shows the all cases and their boundary conditions.

**B. Grid generation**

A high-quality mesh is produced using multi-block H-grid inside the jet pump. This type of grid gives the minimum skew angle, which should not be less than  $20^\circ$ , and the maximum aspect ratio, which should not be more than 100. The total number of grid nodes is about 430 000. To insure that, the number of grid nodes used is sufficient to get convergent solution, an iteration of ‘grid independent solution’ is carried out. Three different grids (212,000, 485,600, and 582,700) are checked for the whole jet pump. The results obtained for the 582,700-grid nodes coincided with the results obtained with grid nodes of 485,600, i.e. the grid nodes of 485,600 is enough to achieve grid independence. Figure 2 shows a sample of the grid used.

**Table (1): Boundary conditions for all cases at  $R=0.25$ ,  $L=7.25$ ,  $\theta_a=5.5^\circ$  at maximum efficiency**

Driving pressure	X	Mp [kg/s]	Ms [kg/s]	Pout [Pa]
1 bar	0	0.9722	0.78611	103332.99
	0.5	0.9722	0.91667	103651.35
	0.75	0.99444	0.95	103579
	1	0.9305	1.0778	103887.5
1.5 bar	0	0.80833	0.65833	105251
	0.5	0.833	0.775	104732
	0.75	0.838	0.966	105195
	1	0.86944	1.186	106149
2 bar	0	0.75	0.7639	105951
	0.5	0.75	0.852	107536
	0.75	0.725	0.941	107225
	1	0.7333	0.96111	106719
2.5 bar	0	0.64	0.68889	107678
	0.5	0.638	0.738	109275
	0.75	0.616	0.758	108273
	1	0.6111	0.80833	108267

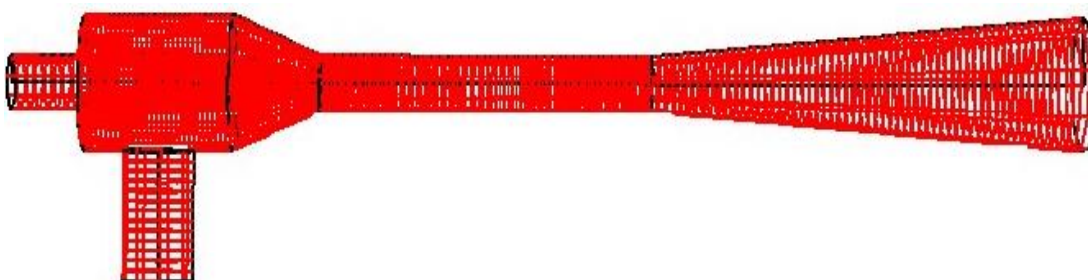


**Fig. (2) Jet pump computational grid system**

**A. Experimental results**

The present experimental results presented here are part of extended program for studying many factors affecting the jet pump performance at the National Water Research Center. In this study, the effect of nozzle to throat spacing to diameter ratio ( $X$ ) on the performance of the jet pump at different driving pressure is discussed. Figure 3 shows the performance curves for  $X=0,0.5, 0.75$  and  $1$  at different inlet pressure of  $1, 1.5, 2,$  and  $2.5 \text{ bar}_{(g)}$  respectively at an area ratio  $R=0.25$ , mixing chamber length to mixing chamber diameter ration  $L= 7.25$  and diffuser angle of  $\theta=5.5^\circ$ . These combinations of geometries are complex to accurately analyze and optimize. Examining these figures, Fig. 3-a, shows that at an inlet pressure of  $1 \text{ bar}$ , the maximum efficiency occurs at a mass flow ratio ranges from  $M=0.5$  to  $0.75$  for the four values of  $X$ . The maximum value of the efficiency occurs at a value of  $X=0.5$ . The same trend is found for driving pressure of  $1.5, 2, 2.5 \text{ bar}$  respectively. From these figures, the maximum efficiency is  $\eta=25\%$  and occurs at  $X=0.5$  where the head ratio is  $N=0.35$  at  $1 \text{ bar}$ , and the minimum value of the efficiency is  $\eta=18 \%$  and occurs at  $X=1$  where the head ratio  $N=0.25$  at a driving pressure of  $2.5 \text{ bar}$ . Examining the figures again, it seems that the value of  $X=0.5$  always gives a slightly better performance. These results agree well with previous study of Cunningham [9] who summarized that  $X$  should be of the order of  $0.5$  to  $1.5$ . and the ESDU design guide [10] which suggested that the nozzle should be placed at a value of  $X=0.5$  to  $1$ . In contrast to these results, Aphornratana and Eames [11] showed very different study for a steam ejector, his optimum  $X$  was found in the range of zero to about  $0.8$  inside the mixing chamber. A similar conclusion of this discrepancy is also found in Cunningham [9]. For an earlier paper Cunningham [5], he reported that  $X$  should decrease within increase in area ratio  $R$ , while three other investigators [7,22,23] found that the optimum value of  $X$  increased somewhat with area ratio. This apparent discrepancy in findings can be rather easily explained on the basis of considerable differences in detailed geometry combination which is almost different from a researcher to another. The detailed flow characteristics and mixing process are needed to be clearly understood for each design. To investigate the effect of ( $X$ ) and the driving pressure on the flow ratio ( $M$ ), Fig. 4 show this relation extracted from Fig. 3 at maximum efficiency point. From the figure, increasing the value of ( $X$ ) increases the mass flow ratio at the maximum efficiency point. That is may be because increasing ( $X$ ) allows larger area for the entrained flow. Increasing the driving pressure, increases also the mass flow ratio at the maximum efficiency point because the pressure energy converted into kinetic energy at the exit of the nozzle that means a lower pressure is obtained at this region where it can entrain more secondary flow.

The effect of ( $X$ ) and the driving pressure on the maximum efficiency is shown in Fig. 5. Examining the figure, the maximum efficiency is always obtained at a value of ( $X=0.5$ ). The maximum efficiency of a value  $25.5$  percent is obtained at a value of driving pressure  $1 \text{ bar}$ . From the above discussion it can be concluded that: if a high entrained flow ratio is required, the value of ( $X$ ) should be higher but this will be affected by a loss of maximum efficiency. Also the general trend shows that increasing the driving pressure increases the flow ratio at maximum efficiency but this will be paid by decreasing the value of maximum efficiency. Figure 3 is shown in Appendix.

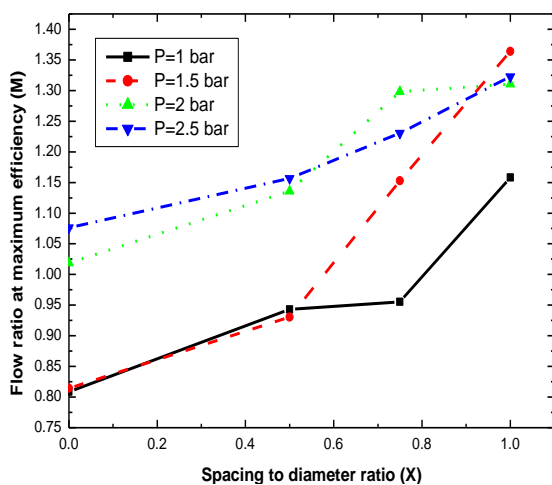


**Fig. 4** Flow ratio at maximum efficiency versus spacing to diameter ratio

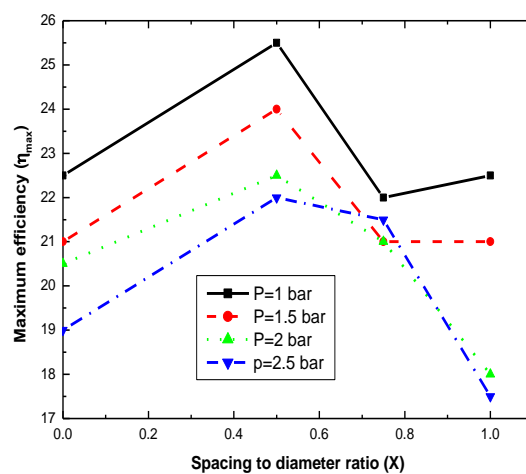


**Fig. 5** Maximum efficiency versus spacing to diameter ratio

**B. Numerical Results**

In this section, the numerical results reflecting the effect of (X) on the velocity profile, mixing process, and pressure distribution are presented and discussed. Figure 6 shows the velocity profile at the nozzle exit section that explains why with increasing the value of (X) the mass flow ratio increases at the maximum efficiency point. Taking the case of driving pressure of P=1 bar as a sample (from Table 1, the other three cases at P= 1.5, 2, 2.5 bar have the same trend of mass flow ratio). Figure 6 shows the relation between local velocity normalized by the average velocity ( $u/U_j$ ) at the exit section of the nozzle at different radial locations ( $r/R_m$ ) for X= 0, 0.5, 0.75, 1 at a driving pressure 1 bar. This figure explains the velocity profile in two important regions. The first one is the flow in the jet region where the velocity profile does not change much for different values of (X) as the inlet pressure is nearly constant at 1 bar and the local velocity reaches a value of zero at the wall of nozzle as shown in the figure. The second region is the suction nozzle region where the entrained flow occurs. The velocity profile is completely different. Increasing the value of (X) increases the area allowed for the entrained flow and hence the entrained flow rate increases at the moment that the primary flow rate does not change much as the inlet pressure is nearly constant.

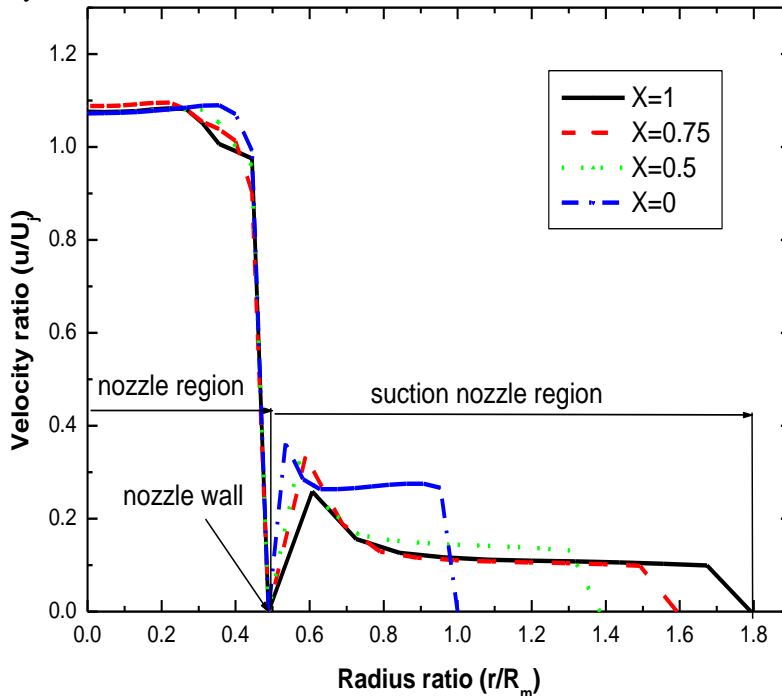


**Fig. 6**Velocity profile at the nozzle exit section at P= 1bar

Figure 7 shows a sample of the velocity contours at the upper middle section along the jet pump at the point of maximum efficiency for (X)= 0,0.5,0.75 and 1 respectively and at 1 bar. The distorted flow from the mixing chamber continues until reaching the diffuser. Quantifying these results, the velocity profile along the mixing chamber is shown in Fig. 8 at some selected sections of the mixing chamber. Figure 8-a shows the velocity profile at the entrance of mixing chamber. From the figure, for (X=0) the profile is more distorted in the area between the jet region and the suction region. For X= 0.5, 0.75, 1, the flow is less distorted. At a radius ratio of ( $r/R_m=0.5$ ) all the local velocities ratios ( $u/U_j$ ) have nearly the same value of 0.71. It should be pointed out that the local velocity at the core of the jet (at the entrance of MC) is higher for the values of X=0.5,0.75 and 1 because the artificial area of the jet is less than the case of X=0. Following the entrance region, at the other section of mixing chamber, mixing of the secondary and primary flows leads to more uniformity in the velocity profile along the mixing chamber. The distortion of the flow at the exit of the mixing chamber is very low. Figure 9 shows an analogy between the flow in the mixing chamber of the jet pump and an ordinary pipe have the same mass flow rate and outlet pressure. From the figure, the velocity profile is much different from the inlet and the outlet of the jet pump due to the entrained flow, but for the ordinary pipe the velocity profile change is very small.

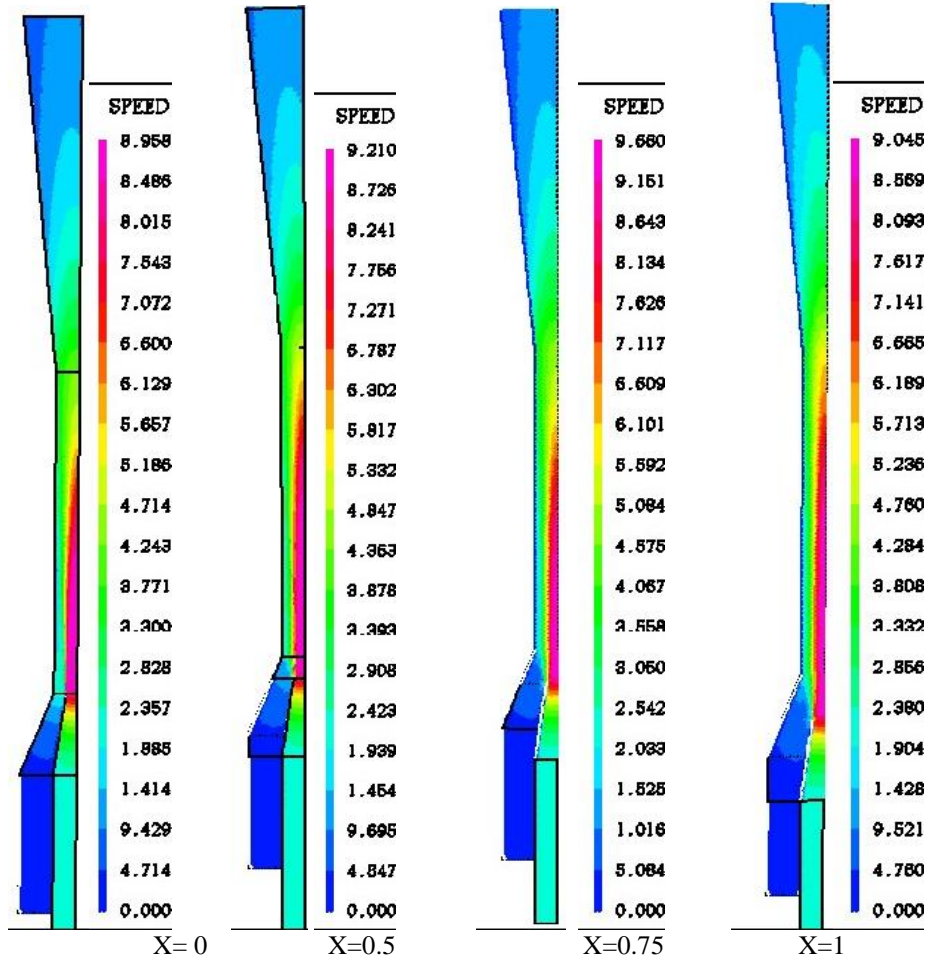


Fig. 7 Contours of velocity magnitude along the jet pump

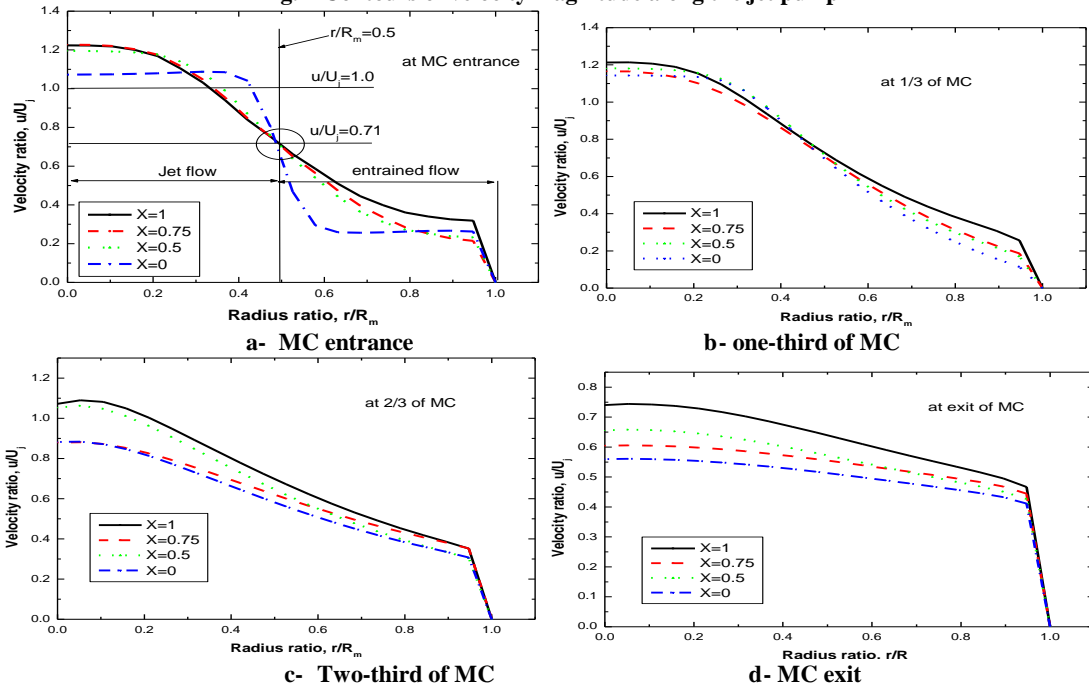


Fig 8 velocity profile at some selected section along the mixing chamber

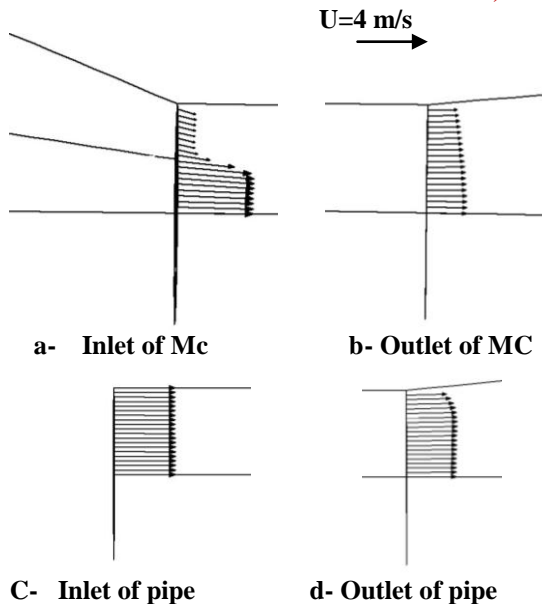


Fig. 9 Analogy between the flow in the MC and the flow in ordinary pipe

One of the important parameters of the jet pump performance characteristic is the pressure coefficient ( $C_p$ ). Figure 10 shows the pressure coefficient along the mixing chamber and diffuser for different values of ( $X$ ). The figure shows that the highest value of ( $C_p$ ) is obtained at a value of  $X=0$ . This confirms the previous findings of Fig.6 where local velocity is higher (for  $X=0$ ) in the suction chamber region because the area is smaller, that will decrease the vacuum pressure in the suction line and hence increases the coefficient of pressure where  $C_p = \frac{P - P_s}{0.5 \rho U_j^2}$ . The higher velocity in the suction chamber is not recommended as it make the pump easy to

cavitate. This result agrees very well with the previous findings of Cunningham [9] and Snager [24]. They did not recommend the value of  $X$  to be zero for the reason of cavitation problems. From the figure also it can be shown that both the mixing chamber and the diffuser share, approximately, equally the pressure coefficient rise.

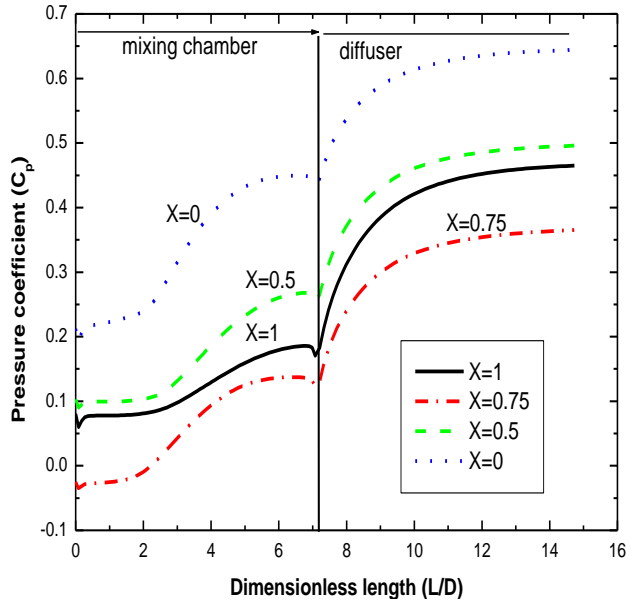


Fig. 10 Pressure coefficient along the mixing chamber diffuser for different values of ( $X$ )

#### IV. COMPARISON BETWEEN EXPERIMENTAL AND NUMERICAL RESULTS

Figure (11-a) shows a sample comparison between the experimental and numerical results of N-M curves, whereas Figure (11-b) shows the corresponding  $\eta$ -M curves at a driving pressure 1 bar for the following configuration: area ratio  $R=0.25$ , mixing chamber length ratio  $L/D=7.25$ , diffuser angle  $\theta=5.5^\circ$  and  $X=0.5$ . From the figure, the numerical curve is slightly higher than the experimental curve. Generally, the matching between them is fairly good, and the flow details, which could not be experimentally obtained inside the pump, are numerically obtained. It is believed that, the small deviation is due to the smoothness of the fittings and pipes. The choice of standard  $k-\epsilon$  model is an acceptable choice with no loss in accuracy compared to the other two equation turbulence models, Fan et al [12].

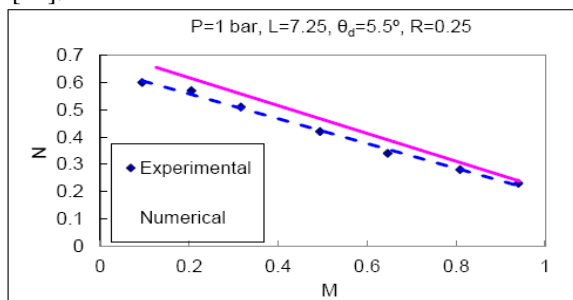


Fig. 11-a

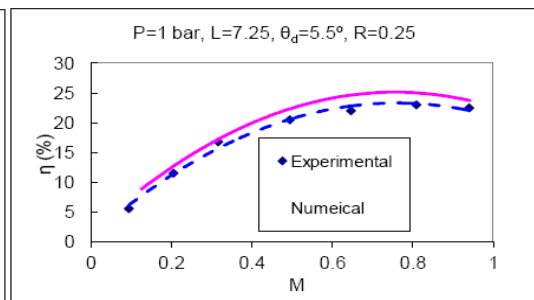


Fig. 11-b

Fig. 11 Comparison between experimental and numerical results



ISSN: 2319-5967

ISO 9001:2008 Certified

International Journal of Engineering Science and Innovative Technology (IJESIT)

Volume 2, Issue 5, September 2013

## V. CONCLUSION

In this study, investigations were done based on the performance of water jet pump. Tests are carried out at different driving pressures  $P=1, 1.5, 2,$  and  $2.5$  respectively. Four values of nozzle -to-throat spacing to mixing chamber diameter ratio. CFX-Tasc flow code is used for the numerical calculations.

The following points are summarizing the important conclusion and the general trend of the performance variables.

1. The optimum value of "X" that gives the maximum efficiency is  $X=0.5$ .
2. Increasing the driving pressure increases the flow ratio at maximum efficiency.
3. Increasing the value of "X" increases the mass flow ratio. The CFD findings are in good agreement with ESDU (1985) guidelines.
4. The value of  $X=0$  is not recommended at all for the reason of cavitation problems.
5. The CFD results obtained (which is difficult to obtain experimentally) is very useful for the designer.

### Nomenclature

$A_J$	= Cross sectional area of the jet, ( $m^2$ )
$A_{mix}$	= Cross sectional area of the mixing chamber, ( $m^2$ )
$D$	= Nozzle (jet) diameter, (m)
$L$	= Mixing chamber length to mixing chamber diameter ration
$P$	= Total pressure = $P_d - P_s$
$P_m$	= Motive pressure, (Pa)
$P_d$	= Discharge Pressure, (Pa)
$\Delta P_o$	= Working pressure of slurry jet pump, (Pa)
$N$	= Head ratio, (-)
$P_s$	= Suction Pressure, (Pa)
$M$	= Flow ratio, (-)
$R$	= Area ratio = $A_J/A_{mix}$ , (area of nozzle to area of mixing chamber)
$R_m$	= Mixing chamber radius
$X$	= Ratio of nozzle-to-throat spacing to mixing chamber diameter ( $x/D$ )
$x$	= Nozzle-to-throat spacing (distance between the nozzle exit and the beginning of the mixing chamber), (mm)
$\gamma$	= Specific weight, ( $N/m^3$ )
$\eta$	= jet pump efficiency = $M \times N$

### Subscripts

$d$	= Discharge
$i$	= Nozzle tip
$_{mix}$	= Mixing chamber
$_m$	= Motive
$_s$	= Suction

### REFERENCES

- [1] J. Thomson "On a jet pump or apparatus for drawing up water by the power of a jet" Report, British Assn., London, England, 1852, pp. 130.
- [2] J.M. Rankine "On the mathematical theory of combined streams "Royal Soc., London, England, 19, 1870, pp. 90.
- [3] H. Lorenz" Technische hydromechanik" R. Oldenburg, Berlin and Munich, Germany, 1910.
- [4] J. Gosline, and O'Brien, "The water jet pump", University of California Publications in Engineering, Vol. 3, No. 3, 1934, pp. 167-190.
- [5] R.G. Cunningham, and W. River "Jet-pump theory and performance with fluid of high viscosity", Trans. ASME, Vol.79, 1957, pp. 1807-1820.
- [6] R. Vogel "Theoretical and experimental investigation of air ejectors", Maschinenbautechnik, Berlin, 5, 1956, pp.619-637.
- [7] N.H.G. Mueller "Water jet pump" J. Hydr. Div., 1964, HY3, pp83-113.
- [8] Y.R. Reddy and S. Kar "Theory and performance of water jet pump". J. Hydr. Div., 1968, HY5, pp1261-1281.
- [9] R.G. Cunningham "Liquid jet pump modeling: Effects of axial dimensions on theory-experiment agreement" 2<sup>nd</sup> Symposium on Jet Pumps and Ejectors and Gas Lift techniques. England. March, 1975, pp. 1-15.





ISSN: 2319-5967

ISO 9001:2008 Certified

International Journal of Engineering Science and Innovative Technology (IJESIT)

Volume 2, Issue 5, September 2013

- [10] ESDU, "Ejector and jet pump" data item 86030, ESDU International Ltd, London, UK, 1985.
- [11] S. Aphornratana, I.W., Eames "A small capacity steam-ejector refrigerator: experimental investigation of a system using ejector with movable primary nozzle", Int. J. Refrig. 20 pp. 352–358, 1997.
- [12] J. Fan , J. Eves, H.M. Thompson, V.V. Toropov, N. Kapur, D. Copley and A. Mincher "Computational fluid dynamic analysis and design optimization of jet pumps" Computers & Fluids 46 (2011) pp.212–217.
- [13] T. Meakhail T. and S. Mikhail "Jet pumps and ejectors, Theory, Performance and Design", SD-65843 Sulzbach/Germany 2010 ISBN: 978-3-929682-48-9.
- [14] M. El Gazzar, T. Meakhail, and S. Mikhail "experimental study of the effect of drag reduction agents on the performance of jet pump" Proc. IMechE, Part A: J. Power and Energy, June, 2006, Vol.220, PP.379–386.
- [15] M. El Gazzar, T. Meakhail, and S. Mikhail "A Numerical study of the flow inside annular jet pump". AIAA, "Journal of Thermo physics and Heat Transfer, October–December 2006, Vol. 20, No. 4, pp.930-932.
- [16] M. El Gazzar, T. Meakhail, and S. Mikhail., "Numerical and experimental study of the influence of drag reduction agent (C.M.C.) on the central jet pump performance"., IMechE ,Part A: J. Power and Energy, 2007, Vol.221,PP.1067–1073.
- [17] T. Meakhail, Z. Yaser , M. Elsallak, S. Abdelhady." Experimental study of the effect of some geometric variables and number of nozzles on the performance of a subsonic air-air ejector" IMechE, Part A: J. Power and Energy.2008, Vol. 222, PP. 809-818.
- [18] T. Meakhail " Experimental and numerical study of the effect of mixing chamber length and area ratio on the performance of a subsonic air-air ejector" Journal of Engineering Sciences, Faculty of Engineering, Assiut University, , Jan, 2009, Vol. 37 , No. 1, pp. 85-99.
- [19] T. Meakhail and T. Ibrahim "Experimental and numerical study of the effect of area ratio and driving pressure on the performance of water and slurry jet pumps" IMechE ,Part C: Journal of Mechanical Engineering Science. 2012, Vol. 226 No. (9), pp 2250 - 2266.
- [20] ASC, "CFX-TASCflow documentation Version 2.9.0" Advanced Scientific Computing, Ltd, Waterloo, Ontario, Canada 1999.
- [21] A. Hemidi , F. Henry, S. Leclaire, J. Seynhaeve, Y. Bartosiewicz " CFD analysis of a supersonic air ejector: part 1: experimental validation of single-phase and two-phase operation". Appl Therm Eng 2009; 29: pp. 1523–1531.
- [22] F. Schulz and K.H. Fasol "Wasserstrahlpumpen zur forderung von flussigkeiten" Springer- Verlag (Vienna). 1958.
- [23] A.G. Hansen and R. Kinnavy "The design of water jet pumps Part-I- Experimental determination of optimum design parameters" ASME paper 65-WA/FE-31, 1965.
- [24] N.L. Sanger " An experimental investigation of several low-area ratio water jet pumps" Journal of Basic Engineering, Trans. ASME, Series D, 92, 1, pp.11-20.

APPENDIX

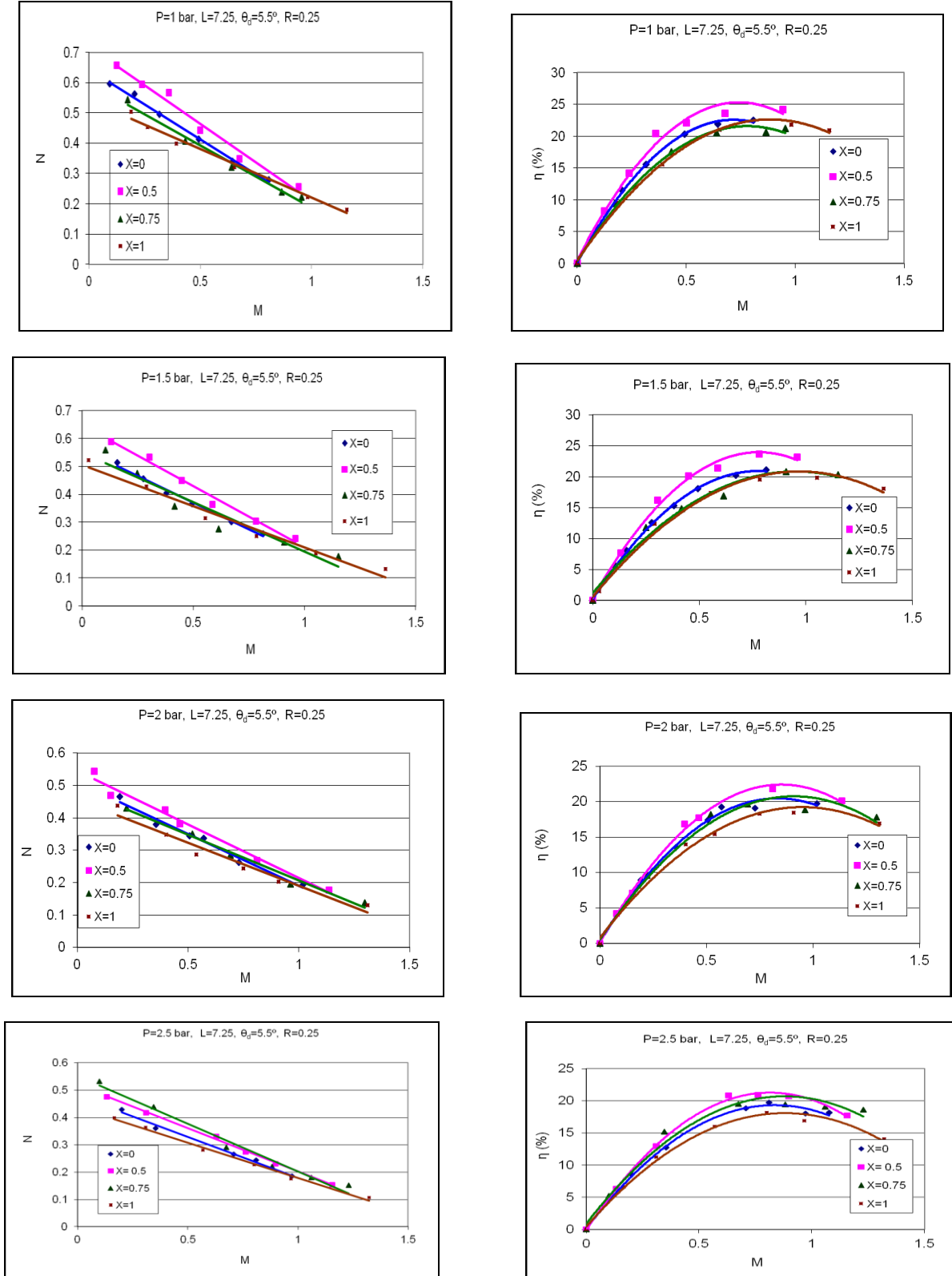


Fig 3 Jet pump performance for different (X) at different motive pressure